OPTIMAL SPECKLE IMAGING OF EXTENDED SPACE OBJECTS - RESULTS FROM FIELD DATA

Charles Matson, Marsha Fox, E. Keith Hege[*], *Laura Hluck, Jack Drummond, David Harvey*[*]

Phillips Laboratory/LIMI
Advanced Imaging Division
Kirtland AFB, NM 87117-5776
USA
E-mail: matson@plk.af.mil

[*] Steward Observatory
University of Arizona
Tucson, AZ 85721
USA

ABSTRACT

Speckle imaging techniques have been shown to mitigate atmospheric resolution limits, allowing near-diffraction-limited images to be reconstructed. Few images of extended objects reconstructed using these techniques have been published, and most of these results are for relatively bright objects. In this paper, we present image reconstructions of an orbiting Molniya spacecraft from data collected using a 2.3 meter ground-based telescope. The apparent brightness of the satellite was 15th visual magnitude. Power spectrum and bispectrum speckle imaging techniques are used prior to image reconstruction in order to ameliorate atmospheric blurring. Optimal weighted least squares estimation methods are used to estimate the Fourier spectrum from the power spectrum and the bispectrum. We demonstrate that these optimal methods produce superior image quality as compared to images created using conventional speckle imaging methods.

1. INTRODUCTION

Astronomical speckle imaging techniques have been demonstrated to provide improved image resolution when using ground-based telescopes as compared to conventional long-exposure imaging. Atmospheric turbulence typically limits image angular resolution to an average of 5-10 μrad, while a 2.3 meter telescope has a diffraction-limited resolution of approximately 0.24 μrad at 550nm. Speckle imaging techniques are post-processing methods used to overcome atmospheric turbulence effects and approach diffraction-limited resolution. In addition to residual atmospheric turbulence noise, detector noise and Poisson noise limit resolution improvements. Optimal speckle imaging methods for mitigating noise distortions in images have been developed [1],[2] and have been demonstrated to provide improved image quality as compared to conventional speckle imaging methods. In these previous papers, the image improvement was demonstrated using several different approaches. Computer simulations of both binary stars and extended objects were used to quantify algorithmic improvements. In addition, field data collected on a binary star was used to demonstrate the noise reduction achieved outside the image support. An important next step in demonstrating the efficacy of these optimal algorithms is to use them on field data of extended objects. Resolvable objects which consist of a small number of delta functions (such as binary stars) have an inherently low space-bandwidth product which makes their reconstruction easier than for true extended objects [3]. Many field data results have been presented which show the usefulness of speckle imaging techniques to remove atmospheric distortions from point-type objects. However, there is interest in using speckle imaging techniques to improve image quality of extended objects such as artificial satellites [4] and asteroids [5]. Few field data results are available, and those that are available are from reasonably bright targets.

In this paper, we present an image of a Molniya satellite which was reconstructed using the previously-derived optimal speckle imaging techniques. This reconstruction is compared to another reconstruction which was obtained using conventional reconstruction methods. The satellite visual magnitude was 15, making it the dimmest extended object, by several orders of

magnitude, to have been successfully reconstructed (to the authors' knowledge). Prior knowledge of the satellite structure was used to create a wireframe model of the Molniya to demonstrate that object orientation and size are accurately reconstructed.

2. ALGORITHM DESCRIPTION

Our algorithms have been previously reported in detail [1],[2], so we will merely summarize them in this section. Speckle imaging methods utilize an ensemble of short exposure (~10ms) images of an object to create average Fourier domain quantities such as power spectra and bispectra. Let $I_n(u)$ be the Fourier transform of the n^{th} short exposure image. Then the average power spectrum is created by calculating the power spectrum of each short exposure image and averaging over the ensemble of data frames. Similarly, the average bispectrum, B(u,v), defined as

$$B(u,v) = E\{I_n(u)I_n(v)I_n^*(u+v)\} \qquad (1)$$

is calculated by averaging the individual short exposure bispectra over the ensemble of data frames, where E{} denotes expected value. The magnitude of the Fourier spectra of the object can be obtained directly from the average power spectrum by taking its square root. However, the phase spectrum must be calculated from the average bispectrum and thus requires more processing. As seen in Equation (1), multiple estimates of the object phase spectrum are available from the bispectrum. Thus, we use a weighted least squares approach to estimating the phase spectrum, where the weights are derived from the sample variances of the estimated bispectrum components. In addition, the bispectrum contains multiple estimates of the object magnitude spectrum. We use a weighted least squares approach to enhance the magnitude spectrum estimate obtained from the power spectrum. Because our algorithm results in biased estimates, with the bias becoming more significant the lower the signal-to-noise ratio (SNR) of the measured data, we choose to use only the higher SNR components of the bispectrum for the magnitude spectrum estimation.

The resulting magnitude and phase spectra calculated using the previously-described methods now have significantly-improved SNRs well beyond the traditional atmospherically-imposed spatial-frequency limits. However, atmospheric effects are still present in the form of strong attenuation of the high spatial frequencies. Therefore, the above processing steps are also carried out for an unresolved star angularly near the object. This allows us to estimate the atmospheric attenuation function and thus remove it using standard deconvolution methods.

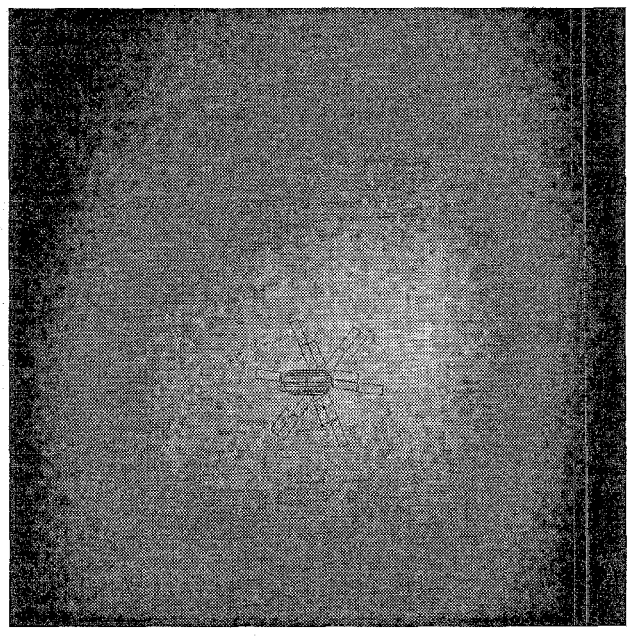

Figure 1. Long exposure image reconstruction of a Molniya spacecraft from 10 minutes of data with an appropriately-scaled wireframe model of the Molniya overlaid.

Conventional speckle imaging methods use the so-called recursive method [1] for phase spectrum estimation. It enables a non-iterative solution to be obtained quickly. The price paid for a non-iterative solution is the restriction that only a subset of the information available in the bispectrum can be used. Our weighted-least-squares approach uses all the available information but requires iteration in order to converge to the correct solution.

3. MOLNIYA RECONSTRUCTIONS

The Molniya satellite [6] is approximately 9 meters in length across the longest dimension of the solar panel array. Its distance from the earth's surface ranges from 500km to 40,000km. The Molniya field data was collected using the Steward Observatory 2.3m telescope on Kitt Peak outside of Tucson, AZ. The camera used to record the data was a photon-counting multiple-anode microchannel-array (MAMA) camera from the Stanford Center for Space and Astrophysics. The observation wavelength was 550nm with a spectral bandpass of 30nm. Ten minutes of data were used to obtain the images. Because the MAMA camera continuously records photon

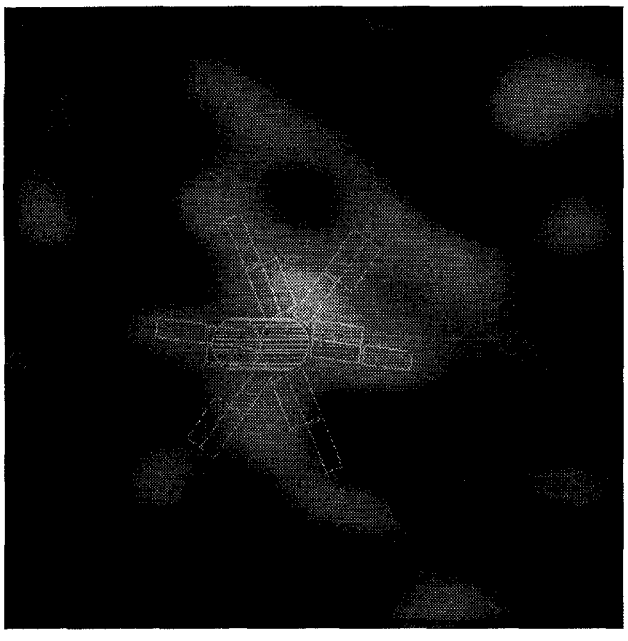

Figure 2. Speckle imaging reconstruction of the Molniya spacecraft using optimal algorithms. The dimensions of this figure and Figure 3 are half that of Figure 1.

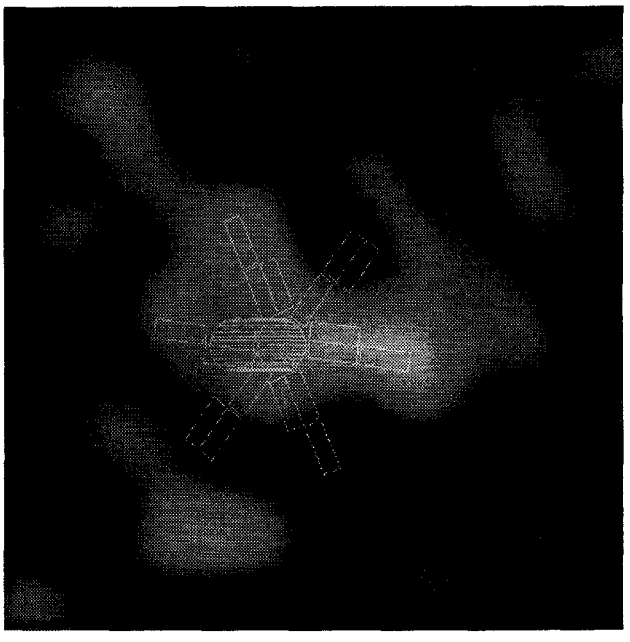

Figure 3. Speckle imaging reconstruction of the Molniya spacecraft using conventional speckle imaging methods.

locations, the short exposures were created after the observation was concluded, and there was no camera readout time causing time delays between the frames. The satellite brightness when we imaged it was approximately m_v=15 and the satellite was at 10,000km.

Figure 1 shows a conventional long exposure image of the satellite obtained using the full ten minute exposure time. A rudimentary wireframe representation of the Molniya spacecraft, scaled to the appropriate size, is shown overlaying the long exposure image. Notice that the satellite is much smaller in size than the resolution afforded by the atmosphere.

Figure 2 is a reconstruction of the satellite using the optimal speckle imaging methods. The sun's illumination is coming from the upper left of the image, out of the page. As a result, the satellite body, which extends out of the plane of the paper, is shadowing the lower solar panels, resulting in incomplete reconstruction of them. Notice that we have reconstructed the satellite morphology accurately enough to determine the satellite's orientation and size. For the image in Figure 2, we used the weighted-least-squares algorithms for both the phase and magnitude spectrum estimation. Because of the low SNR of the bispectral components, the bispectrum weighted-least-squares enhancement of the power-spectrum-derived magnitude spectrum was minimal. We noticed a significant improvement in image quality when using the weighted-least-squares phase spectrum estimate, however.

The reconstruction of the satellite using conventional speckle imaging methods (i.e., the recursive approach to phase spectrum estimation from the bispectrum and using only the direct power spectrum estimate to calculate the magnitude spectrum) can be seen in Figure 3. Notice that we can only reconstruct part of the satellite morphology - not enough to determine what kind of satellite it is or what its orientation is. The wireframe overlaying the image was oriented using the reconstruction in Figure 2. By using this previously-oriented wireframe model, we can see that some features of the Molniya show up in this reconstruction, even though it does not have the image quality of the reconstruction in Figure 2. In addition, the optimal reconstruction has mean square noise levels a few percent lower than the reconstruction in Figure 3.

4. CONCLUSIONS

The optimal speckle imaging algorithms we have developed were used to reconstruct an image of an orbiting Molniya spacecraft. We have demonstrated that the use of these optimal algorithms result in improved image quality as compared to image reconstructions using

conventional speckle imaging algorithms. When using low SNR bispectrum data, only phase spectrum estimates benefit noticeably from the use of the optimal algorithms.

For the Molniya spacecraft, image morphology could only be reconstructed when the optimal algorithms were used. The image obtained when using the optimal algorithms provided enough detail to determine satellite orientation and size.

5. ACKNOWLEDGMENTS

The authors' wish to express their appreciation to J.S. Morgan (currently on staff in the astronomy department at the University of Washington, Seattle, Washington, USA) for providing and operating the MAMA camera used for the data collection.

6. REFERENCES

[1] C.L. Matson, "Weighted-least-squares phase reconstruction from the bispectrum," J.Opt.Soc.Am.A, vol.8, pp.1905-1913 (1991)

[2] C.L. Matson, "Weighted-least-squares magnitude-spectrum estimation from the bispectrum," J.Opt.Soc.Am.A, vol.8, pp.1914-1921 (1991)

[3] C.L. Matson, "Fourier spectrum extrapolation and enhancement using support constraints," IEEE Trans. Sig. Proc., vol.42, pp.156-163 (1994)

[4] T.W. Lawrence, J.P. Fitch, D.M. Goodman, N.A. Massie, R.J. Sherwood, and E.M. Johansson, "Extended image reconstruction through horizontal path turbulence using bispectral speckle interferometry," Opt.Eng., vol.31, pp.627-636 (1992)

[5] J. Drummond, A. Eckart, and E.K. Hege, "Speckle interferometry of asteroids", Icarus, vol.73, pp.1-14 (1988)

[6] Jane's Spacecraft Atlas (1989)